NUKLEONIKA 2006;51(1):85–92



# High kinetic energy dense plasma jet

**Alexander V. Voronin,**
**Vasily K. Gusev,**
**Yury V. Petrov,**
**Nicoliy V. Sakharov,**
**Klara B. Abramova,**
**Kurt G. Hellblom**

**Abstract** Researches on the plasma jet source and injection of hydrogen plasma and neutral gas jets into the Globus-M spherical tokamak are presented. A novel source of dense plasma with high directed velocity is designed, constructed and investigated. This is a double stage system consisting of an intense source utilizing titanium-hydride grains for neutral gas production and a conventional pulsed coaxial accelerator. Optimization of the accelerator parameters, so as to achieve a maximum possible flow velocity with a limited discharge current and a reasonable length of the coaxial electrodes is performed. The calculations are compared with the experiment. A test bed is used for investigation of the intense plasma jet generated by a plasma gun. Plasma jet parameters, among them pressure distribution across the jet, flow velocity, plasma density etc., were measured. Plasma jets with densities of up to $10^{22}$ m$^{-3}$, total numbers of accelerated particles (1–5) $\times$ $10^{19}$, and flow velocities of 50–100 km/s were successfully injected into the plasma column of the Globus-M tokamak. Interferometric and Thomson scattering measurements confirmed a deep jet penetration and a fast density rise (<0.5 ms) at all spatial points up to the radius $r \approx 0.3a$. The injection did not result in plasma degradation.

**Key words** plasma gun • spherical tokamak • fuelling system

A. V. Voronin✉, V. K. Gusev, Yu. V. Petrov,
N. V. Sakharov, K. B. Abramova, K. G. Hellblom
A. F. Ioffe Physico-Technical Institute,
26 Politechnicheskaya Str.,
194021 St. Petersburg, Russia,
Tel.: +7 812 2479121, Fax: +7 812 2471017,
E-mail: voronin.mhd@mail.ioffe.ru

Received: 25 August 2005
Accepted: 30 December 2005

## Introduction

The development and production of gas or plasma jets with a high kinetic energy is an issue with a fundamental and applied potential. Specifically, the problems of plasma fuelling and density profile control are topical for any high-performance magnetic-trap operation. Of particular importance for the operation of a future thermonuclear tokamak-reactor is the development of efficient plasma fuelling methods. The fuel must have a high enough directed energy to pass through the dense and hot plasma border prior to reaching the central plasma region. The total number of accelerated particles has to be $10^{19}$–$10^{23}$ for densities $>10^{21}$ m$^{-3}$ and flow velocities of up to 800 km/s. Fuelling of fusion plasma by gas puffing, while being a cheap and reliable technique, has a low efficiency. Significant progress was reached in the pellet injection technology [4, 8]. Being fundamentally limited by the pellet velocity, such injection is, however, hardly an adequate approach to fuelling central regions in tokamak reactors. Neutral beam injection [5] proved successful in producing high-temperature and high fusion performance plasmas, nevertheless, this expensive method requires further increase of beam energy up to the MeV range before it is accepted for reactor fuelling. Collective acceleration of magnetically confined plasma rings (compact tori) [9] was proposed for central fuelling of tokamak plasma. There is a limit on its density. A possible candidate, made promising by the achievement of high flow

velocities, is directed injection of a plasma jet [7]. Most of the present-day plasma guns are capable of accelerating relatively low-density plasmas only. No guns that could generate dense, highly ionized and pure plasma jets with a high directed velocity have thus far been demonstrated. Research carried out at the Ioffe Physico-Technical Institute has culminated in the development of a fuelling method and of a prototype of a pulsed accelerator producing an intense, dense hydrogen (eventually deuterium) plasma jet [11].

## Working principal and monitoring

A novel source of dense plasma with high directed velocity is designed, constructed and investigated. The principals of operation are basically described in [11]. The source consists of two stages (Fig. 1). The first (gas generating) stage contains titanium grains loaded with hydrogen. Intense electric discharge passing through the grains releases a gas cloud. This neutral gas (hydrogen) passing through the specially designed grid fills the gap between the electrodes (the second stage) up to thousands atmospheres in few microseconds. This is one of the principal distinguishing features of the design, helping in achievement of compact or dense plasma cluster. The second stage is the plasma generating. Intense electric discharge through the gas between the coaxial electrodes provides gas-ionization and plasma-acceleration in a classical "Marshall gun scenario". Both stages of the source are connected to low inductance capacitor power supplies. The source was composed of: $C_1 = 20$ μF, $U_1 \le 6$ kV, $C_2 = 40$ μF, $U_2 \le 10$ kV. The circuits were switched by ignitrons. Care was taken to minimize inductances of the discharge circuits and the highest power input into the jet. The integral parameters of dense magnetized plasma (DMP) jet produced by the double stage source were

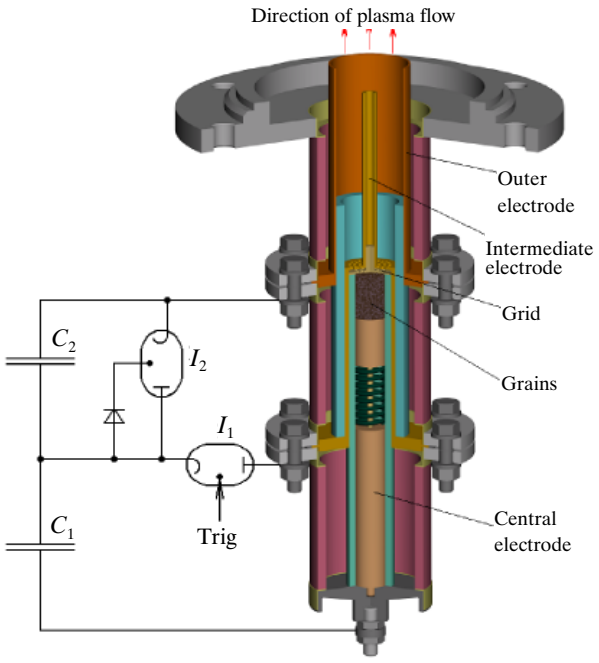


**Fig. 1.** Double stage plasma source.

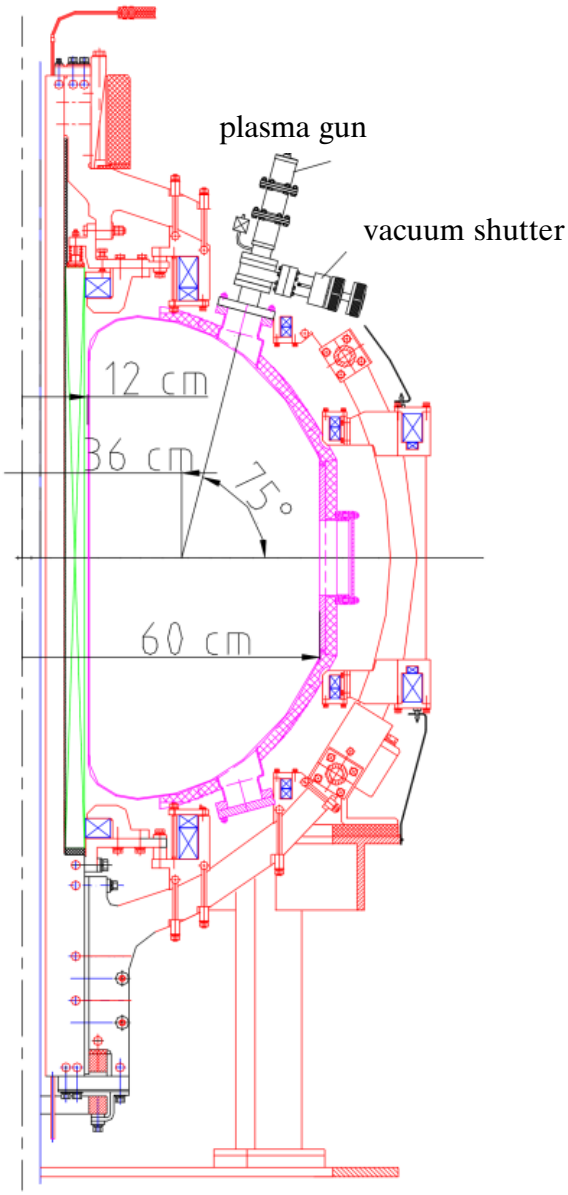


**Fig. 2.** Plasma source placed at the spherical tokamak Globus-M.

measured. They are: average density of plasma jet $10^{22}$ m$^{-3}$; total number of particles in one jet (during 50 μs) $5 \times (10^{18} \div 10^{19})$; jet speed range 15–70 km/s. The efficiency of ionization reached 90%.

A basic investigation was performed of the possibility of controlling the processes in tokamak plasma with an external source generating dense plasma flux [1]. The source was mounted on the Globus-M vacuum vessel flange with a vacuum shutter (Fig. 2). A description of the design, operational principles, and experimental program of Globus-M can be found in [3]. The basic design characteristics are as follows: aspect ratio $A = R/a = 1.5$, major plasma radius $R = 36$ cm, minor plasma radius $a = 24$ cm, toroidal magnetic field at the vessel axis $B_T = 0.2$–$0.5$ T, plasma current $I_p = 0.1$–$0.35$ MA, average plasma density $n_e = (1–7) \times 10^{19}$ m$^{-3}$, pulse duration with inductive current drive $\tau_{pulse} \le 0.12$ s.

Two applications of plasma jet injection have been studied. The first one was the plasma discharge initiation.

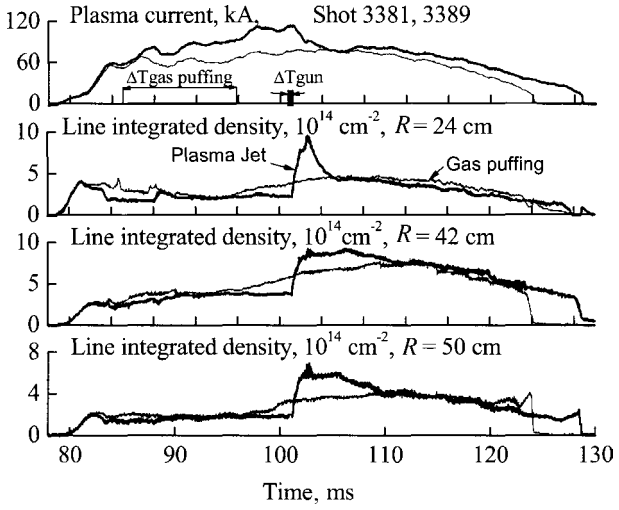


**Fig. 3.** Plasma injection (bold lines) and gas puffing (thin lines) at the plateau discharge current.

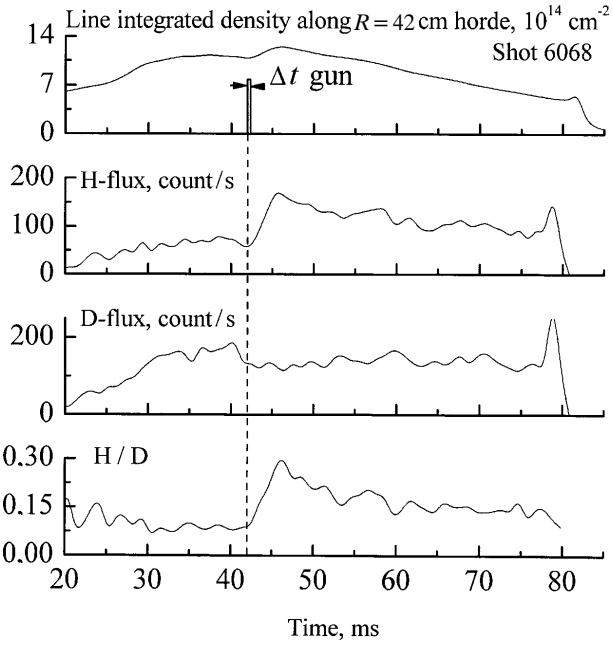


**Fig. 4.** Evolution of hydrogen in deuterium plasma. Flux energy 470 eV.

The DMP jet was injected into camera during the breakdown phase instead of RF pre-ionization and vacuum vessel pre-filling with working gas. Plasma current ramped up faster and to a higher value at the same loop voltage wave form, magnetic turbulence during current ramp-up was lower, plasma density reached a higher value; background radiation of $H_\alpha$ line was lower than with gas-puffing and pre-ionization system. The second application was the plasma density regulation. The hydrogen jet was injected in deuterium plasma during current plateau. The observation of the injected plasma radiation into the vacuum magnetic field helped to estimate the possible penetration depth of plasma jet into the main plasma. The speed of the jet was 30 km/s: the deeper penetration of plasma jet with equal velocities conforms to a lower magnetic field. The plasma jet seems to be stopped by the magnetic field value below 0.25 T in the vessel center (the field at the gun nozzle position is about 0.2 T). Some results of plasma measurements are displayed in Fig. 3. It is seen an increase of the plasma average density. The density rose up during 1–2 ms following the gunshot. Injection of the plasma jet led to a faster increase of the plasma density compared with gas puffing (more than 15 ms). Measurements of plasma density profile by means of a multichannel radar-reflectometer revealed an increase of density gradient not only near the plasma periphery but also inside the plasma volume. The time evolution of the hydrogen charge-exchange flux in deuterium plasma, recorded by a neural particle analyzer is presented in Fig. 4. It is seen that the fraction of hydrogen flux rose up with increasing plasma density during 1÷2 ms after jet injection. Maximum flux of hydrogen was at the energy 470 eV. Percentage of the hydrogen increased in deuterium plasma up to 25%. It means that injected plasma penetrated into hot plasma body. Dense plasma jet being injected into the tokamak plasma does not deteriorate main plasma properties; this means it does not induce impurities or initiate MHD perturbations. This may be attributed to pure plasma produced with such a plasma source, operating at very high neutral gas pressure (minimum pulse duration to collect required total amount of particles) and low accelerator current densities, which do not erode electrode materials.

The performed experiments have demonstrated the applicability of plasma jet for plasma density regulation and for the discharge breakdown instead of RF pre-ionization and gas puffing. But for the effective employment, the source has to be developed to produce a plasma jet with a higher kinetic energy and with an as low as possible impurity content. According to theoretical consideration of flight of constant mass between coaxial electrodes with capacitor power supply [6], the velocity of flow can be increased.

## Optimization of the second stage

### Numerical model

Numerical simulation was used to analyze the acceleration process in a coaxial accelerator with a variable capacitor battery restricted by the condition of fixed energy conservation at zero losses [10]. Electrodynamic plasma acceleration along with the $z$ axis can be described in the simplest case by the coupled equations of Arcimovich [2]:

$$m_0 \frac{d^2 z}{dt^2} = \frac{I^2}{2} \frac{dL}{dz},$$

$$I = -C_0 \frac{dU}{dt},$$

$$\frac{d(LI)}{dt} = U,$$

$$L = L_0 + bz.$$

Here: $t$ is the time; $m_0$ is the mass undergoing acceleration which we assume constant; $I$ is the current

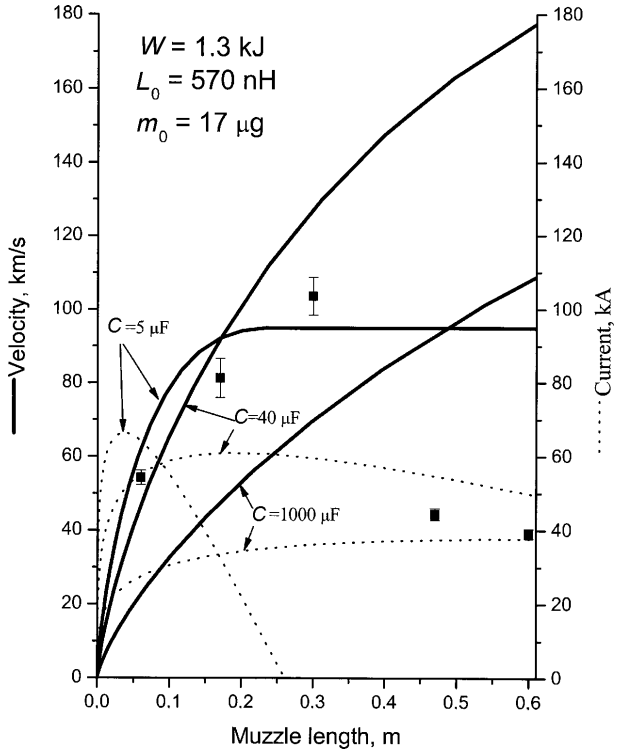


**Fig. 5.** Evolution of plasma velocity and discharge current distribution along muzzle length. Squares with the error bars represent experimental velocity values for the gun with $C_2$ = 40 μF power supply.

through the circuit; $C_0$ is the battery capacitance; $U$ is the voltage between the electrodes; $L_0$ is the initial circuit inductance, and $b$ is the distributed inductance per unit length of the path of the accelerating mass. The ohmic resistances of the electrodes and of the plasma are neglected. The above system was solved numerically by the fourth-order Runge-Kutta method for the particular case of finite coaxial electrode lengths and unipolar current wave form.

The evolution of the plasma velocity (solid lines) and discharge current (dot lines) along the muzzle is displayed in Fig. 5 for different capacitances. A simulation reveals that the highest velocity can be attained with the largest capacitance and a long enough muzzle. The length of the coaxial electrodes is, however, practically limited to ~ 1 m. We readily see that the highest current for a limited electrode length is reached near either the inlet to ($C_2$ = 5 μF) or the outlet ($C_2$ = 1000 μF) from the muzzle, which places a constraint on the output jet velocity. Peaked power deposition along the path of the accelerating mass may also bring about high impurity content. The simulation suggests that in order to achieve a maximum plasma jet velocity for a given stored energy and limited muzzle length, the current layer amplitude along the whole length of the muzzle should be as large as possible. This is the case of intermediate capacitance (e.g., $C_2$ = 40 μF). Experimental measurements of the plasma jet velocity were carried out on the test bed for different muzzle lengths. The experimental points in Fig. 5, while following correctly the pattern of the theoretical curve up to muzzle lengths of 0.3 m, lie below the calculated values, apparently because of the model not including the losses. The strong discrepancy between experiment and simulation for longer muzzles remains unclear but could be attributed to some disregarded factors, in particular, minor design flaws. Further experiments were conducted with close to optimum parameters of coaxial accelerator length and power supply (muzzle length 0.3 m, $C_2$ = 40 μF).

## Test bed experiments

The parameters of intense plasma jets were studied by use of an experimental test bed (Fig. 6). Optimized plasma source (muzzle length 30 cm, outer electrode diameter 35 mm, $C_2$ = 40 μF) was mounted on the vacuum chamber whose volume is 2 m$^3$. The plasma density was measured with a He-Ne laser interferometer. A movable piezoceramic probe measured the pressure profile and total kinetic energy of the jet. The $H_\alpha$ and $H_\beta$ hydrogen lines were isolated with a two-channel spectrometer. The flow velocity was measured with two collimated PM tubes recording the light near the gun edge and at the opposite wall of the vacuum chamber. A CCD camera registered time-integrated radiation emitted by the jet. The discharge current distribution (or voltage drop visualization) along the muzzle was followed with a number of special current shunts connected to different parts of the coaxial accelerator outer electrode. A permanent movable C-magnet (5 cm gap) was mounted beyond the gun edge to separate neutrals from the charged particle flow.

The evolution of plasma gun parameters measured on the test bed is displayed in Fig. 7. The outlet current is delayed with respect to current at the inlet. This implies that the current layer reaches the gun outlet. The plasma jet velocity varied with discharge current in the gun and was measured by recording time delays between the corresponding signals. The measured

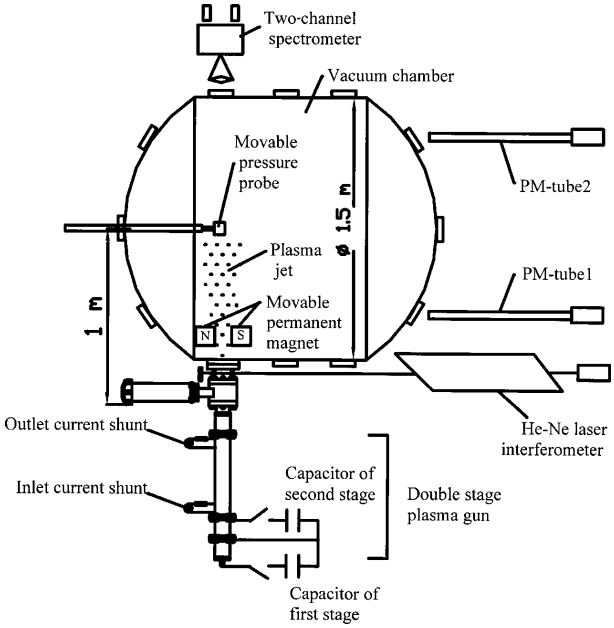


**Fig. 6.** Test bed for investigation of the plasma gun.

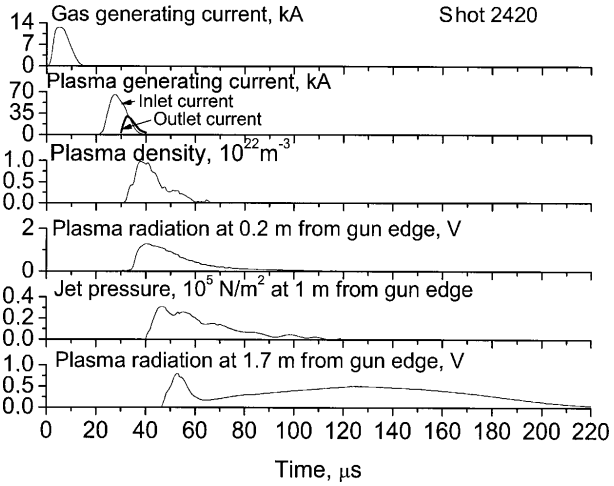


**Fig. 7.** Waveforms of the plasma gun parameters.

plasma jet velocity did not deviate from calculations by more than ~ 25%. The deviation may be attributed to the energy dissipation in the electric circuit (the amplitude and duration of the outlet current are smaller than those of the inlet). The time-integrated jet radiation recorded by the camera shows a directed, sharp-boundary jet, with a diameter of ~ 10 cm at a distance of 1 m from the source edge. The plasma temperature of the jet is of the order of ~ 1 eV. It was derived from the measured $H_\alpha/H_\beta$ line intensity ratio assuming a Boltzmann energy distribution. The pressure profile of the jet was determined with a movable pressure probe at a distance of 1 m from the source edge (Fig. 8). We see that the energy flow is concentrated near the jet axis within a ~ 10–15 cm diameter. The measurements of the jet divergence gave approximately the same value of the jet temperature as the spectroscopic measurements. The temperature was derived from a comparison of transverse and directed kinetic energies of the jet. The kinetic energy of the jet is as high as 100–500 J (for a stored capacitor energy of 0.65–1.3 kJ). The energy was estimated as $W = N \cdot m_p \cdot V^2/2$, where $N = (1–5) \times 10^{19}$ is the number of accelerated particles (as derived from He-Ne laser interferometer data and plasma volume evaluation); $m_p$ is the proton mass;

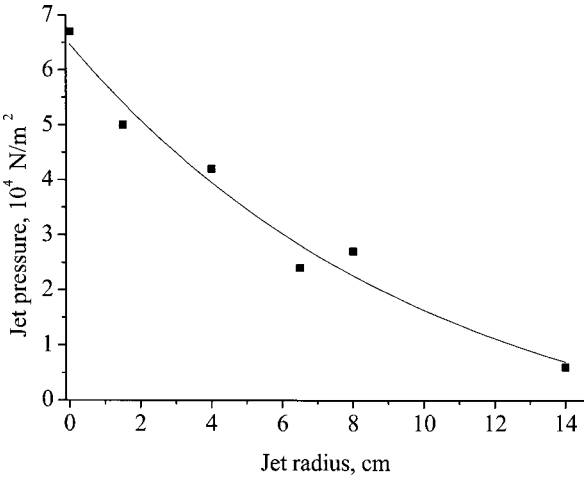


**Fig. 8.** Plasma jet pressure radial distribution measured at 1 m from the gun edge. Initial jet velocity is 100 km/s.

$V$ ~ 110 km/s is the measured velocity. An optimized source generated during ≤ 50 μs pure, highly ionized hydrogen plasma jet with a density up to $10^{22}$ m$^{-3}$, total number of accelerated particles $(1–5) \times 10^{19}$, and a flow velocity of 50–110 km/s.

We studied jet penetration across transverse magnetic field generated by the movable magnet near the gun edge. The radiation of the jet crossing a magnetic field of 0.3 T can be viewed in Fig. 9. No visible radiation

$B$ = 0.3 T, view perpendicular to the source axis

$B$ = 0.3 T, view along to the source axis

**Fig. 9.** Radiation of the plasma jet passing the transverse magnetic field.

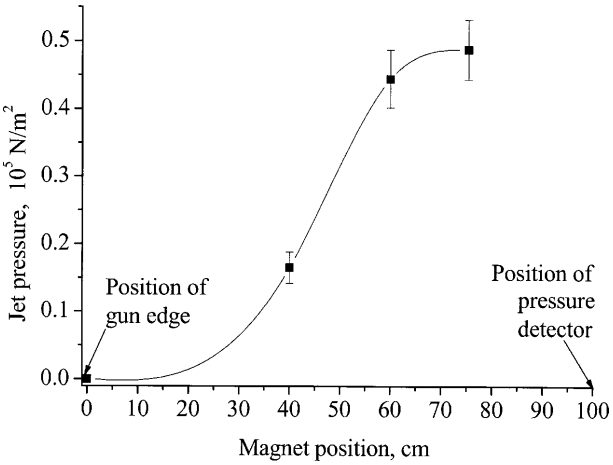


**Fig. 10.** Plasma jet pressure plotted vs. distance between the permanent magnet (strength $B$ = 0.3 T) and the plasma gun edge. Initial jet velocity is 75 km/s.

was detected beyond the magnet. As expected, the magnetic field stops the injected plasma if its specific kinetic energy or pressure is lower than the pressure of the transverse magnetic field. In this particular case of a magnetic field of 0.3 T, plasma flow velocity of 50 km/s, and density $\leq 10^{22}$ m$^{-3}$, the pressure measured beyond the magnet was found to be near zero. The magnetic field was varied in the 0.0–0.3 T interval with the magnet fixed in position. The jet pressure was recorded with a piezoceramic probe located beyond the magnet. The pressure decreases with increasing magnetic field.

The dependence of jet pressure on the distance between the permanent magnet ($B$ = 0.3 T) and the gun edge is presented graphically in Fig. 10. In this experiment, the piezoceramic probe was located at a distance of 1 m from the gun edge and recorded full pressure amplitude (~ 0.5 atm) from plasma jet moving with velocity of 75 km/s at zero magnetic field. Then, the magnet was placed between the gun and the pressure probe to create transverse to the plasma jet magnetic field. Measurements were taken at different magnet positions and constant jet velocity when the magnet was moved between the gun edge and the probe location. It is seen that the jet pressure increases with increasing distance between the gun edge and the magnet, and at a distance of 75 cm reaches the same pressure value as it was without any magnetic field.

## Jet injection into the Globus-M spherical tokamak

In the previous campaigns on the plasma jet interaction with the magnetic field and plasma of Globus-M the plasma jet velocity did not exceed 70 km/s. During recent experiments plasma jet was injected into Globus-M from the equatorial plane, along the major radius from the low field side. The jet speed was increased up to 110 km/s. Another distinguishing feature of recent experiments is that injection was performed at high plasma current amplitude range 200–250 kA at the quasi-stationary discharge phase. The toroidal magnetic field was changed in the range

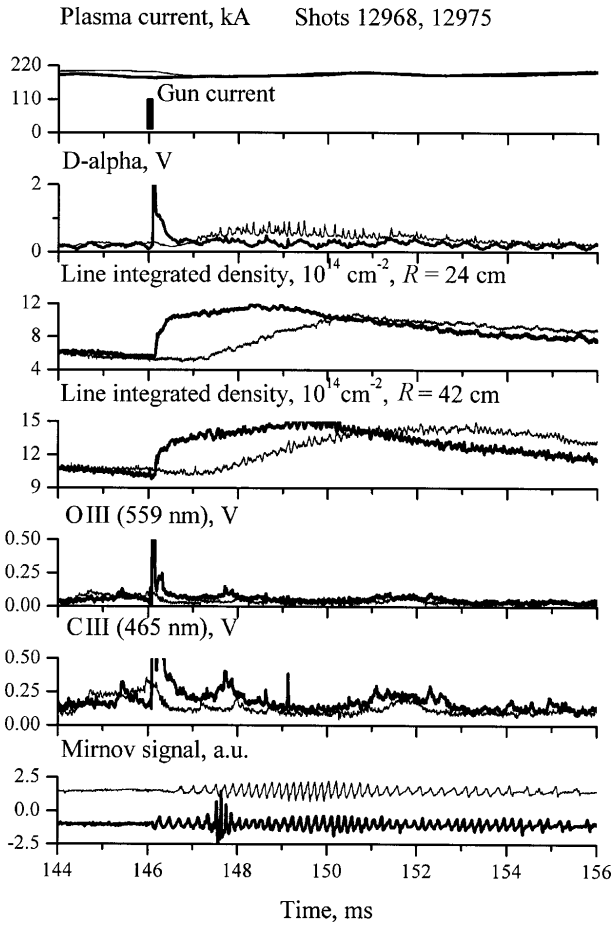


**Fig. 11.** Waveforms of plasma discharge parameters in Globus-M under gas jet (thin lines) and plasma jet (bold lines) injection.

0.3–0.4 T. The line-integrated plasma density was measured with a 1 mm interferometer along three vertical chords at $R$ = 24, 42, and 50 cm. A bolometer recorded radiation losses and a spectrometer was used to detect the $H_\alpha$ radiation, as well as the carbon and oxygen impurity lines.

Figure 11 (bold curves) demonstrates a fast density rise (<0.5 ms) recorded by the interferometer along the peripheral ($R$ = 24 cm) and central (42 cm) chords. In this case, the density rise time was shorter than the diffusion time, and it could roughly be identified with the time necessary for injected particles to equilibrate along the field lines. While the plasma particle inventory increased by 50% (from $0.65 \times 10^{19}$ to $1 \times 10^{19}$), it did not result in plasma degradation (as, e.g., a drop in plasma current, contamination by impurities, MHD activity enhancement). Initial short peaks recorded by $H_\alpha$, OIII, CIII detectors are due to strong backbody radiation of the jet illuminating the vessel interior. After time interval of 2–3 ms all the signals, including bolometer and Mirnov signals returned to the initial (before injection) level. The first measurements of the electron density evolution in these experiments were conducted by the Thomson multi-pulse scattering diagnostics (Fig. 12). Preliminary data suggest that 0.5 ms after the plasma gun shot, the density increases at all spatial points up to the radius $r \approx 0.3a$, thus evidencing

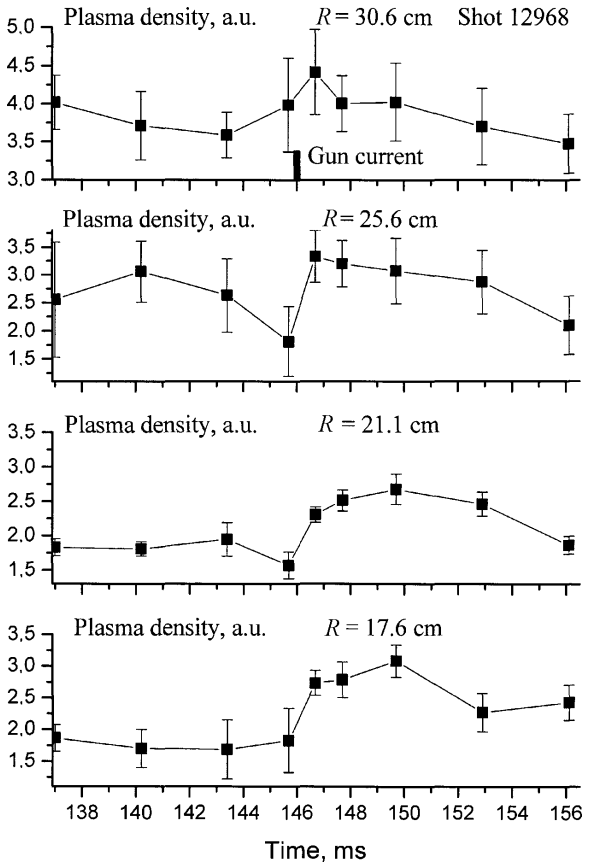


**Fig. 12.** Electron density evolution at different spatial points of the plasma column as derived from multi-pulse Thomson scattering diagnostics. The geometric axis of the column is at $R = 33$ cm.

deep plasma jet penetration. The decrease of the toroidal field from 0.4 to 0.3 T and the plasma current from 200 to 120 kA did not lead to better (faster and deeper) penetration of the plasma jet into the tokamak plasma as may be expected.

To compare the efficiency of plasma jet injection with gas jet, experiments were conducted with the first stage of the plasma gun used as gas generator. Test bed experiments showed the first stage to generate a fairly fast (1–5 km/s) neutral gas jet. This jet was injected into Globus-M and penetrated efficiently into the toroidal magnetic field. The density rise time of ~ 2.5 ms was observed (Fig. 11, thin curves). It is shorter than that achieved customarily with conventional gas puffing (4–5 ms), but being much longer than that characteristic of plasma jet injection (<0.5 ms).

## Discussion

The test bed experiment with plasma jet penetration across a transverse magnetic field demonstrated that an injected plasma jet is indeed stopped by a magnetic field if its specific kinetic energy or pressure is lower than the pressure exerted by the magnetic field. A consequence is that the magnetic field of 0.4 T will stop the plasma jet with a flow velocity ~ 100 km/s and density of $10^{22}$ m$^{-3}$. During experiments on the tokamak, direct measurements of the velocity were not performed. The real velocity of the plasma jet injected into the tokamak plasma may be even lower than measured at the test bed. It is due to braking of the plasma jet by the poloidal magnetic field during accelerating process in the plasma gun closely located to the tokamak. Nevertheless deep jet penetration into the plasma column of Globus-M with toroidal magnetic field of 0.4 T and a fast density increase in the core plasma region was observed. Interferometer and Thomson scattering measurements confirmed deep jet penetration, fast density rise (<0.5 ms) in all spatial points up to the radius $r \approx 0.3a$. This experiments with significantly decreased magnetic field did not show the deeper jet penetration into tokamak plasma. That means that the ratio of specific kinetic energy of the jet to magnetic field pressure does not play exceptional role in the interaction between the plasma jet and tokamak plasma confined by the magnetic field. There is other or additional mechanism of the tokamak density increase during the jet injection.

The efficiency of plasma jet penetration into the magnetic field depends on the number of high-velocity neutrals it contains. This is supported by test bed experiments. We may recall that the jet velocity in these experiments was ~ 75 km/s, and the density measured at the gun edge, ~ $10^{22}$ m$^{-3}$. The transverse magnetic field of 0.3 T does not stop the jet that has passed a distance in excess of 75 cm. At the same time, recombination of the plasma jet to form the jet of neutrals appears the most likely candidate for the process resulting in efficient penetration of particles into the magnetic field.

At the current stage of research, we could not quantitatively separate the contribution of plasma jet and neutral jet components into the density raise effect recorded during injection experiments. New experiments are required.

From experiments performed, we can conclude that our non-sophisticated double stage plasma gun, producing plasma jet with 50 μs duration, density $10^{22}$ m$^{-3}$, total number of accelerated particles $> 10^{19}$ could increase plasma particle inventory in Globus-M by ~ 50% (from $0.65 \times 10^{19}$ to $1 \times 10^{19}$) in a single shot without target plasma parameters degradation.

**Acknowledgment** The authors wish to thank personally Dr. R. G. Levin for his help in equilibrium data processing, Dr. I. P. Shcherbakov, E. M. Sklyarova, S. Yu. Tolstyakov, F. V. Chernyshev for the assistance in calculations and experiments, Dr. A. B. Mineev for valuable comments and discussion and to thank the scientific, technical and engineering staff of the Globus-M tokamak and MHD Phenomena Laboratory of A. F. Ioffe Institute. The authors wish to thank the IAEA for a grant support, Research Contract No. 12408 and RFBR No. 04-02-17606, 03-02-17659.

## References

1. Abramova KB, Voronin AV, Gusev VK *et al.* (2005) Injection of high-density plasma into the Globus-M spherical tokamak. Plasma Phys Rep 31:721–729

2. Arcimovitch LA, Lukyanov SYu, Podgorny IM, Chuvatin SA (1957) Electrodynamic acceleration of plasma clusters. Soviet Journal of Experimental and Theoretical Physics 33:3–8
3. Gusev VK, Burtseva TA, Dech AV *et al*. (2001) Plasma formation and first OH experiments in the Globus-M tokamak. Nucl Fusion 41:919–925
4. ITER Physics Expert Group on Divertor, ITER Physics Expert Group on Divertor Modelling and Database and ITER Physics Basis Editors (1999) Chapter 4: Power and particle control. Nucl Fusion 39:2391–2469
5. ITER Physics Expert Group on Energetic Particles, Heating and Current Drive and ITER Physics Basis Editors (1999) Chapter 5: Physics of energetic ions. Nucl Fusion 39:2471–2495
6. Kolesnikov PM (1971) Electrodynamic acceleration of plasma. Atomizdat, Moscow
7. Marshall J (1960) Performance of a hydromagnetic plasma gun. Phys Fluids 3:134–135
8. Milora SL, Houlberg WA, Lengyel LL, Mertens V (1995) Pellet fuelling. Nucl Fusion 35:657–754
9. Raman R, Martin F, Haddad E *et al*. (1997) Experimental demonstration of tokamak fuelling by compact toroid injection. Nucl Fusion 37:967–972
10. Voronin AV, Gusev VK, Petrov YuV *et al*. (2005) High kinetic energy plasma jet generation and its injection into the Globus-M spherical tokamak. Nucl Fusion 45:1039–1045
11. Voronin AV, Hellblom KG (2001) Generation of dense plasma clusters with high velocity. Plasma Phys Controlled Fusion 43:1583–1592